HAQT deliverable 4-2: Recommendations for new AQ observations to improve AQ situational awareness

Paasonen, P.[1], Timonen, H.[2], Saukko, E.[3], Laakso, M.[4], Shahriyer, A.[1], Kangasluoma, J.[1], Luoma, K.[1], Kuula, J.[2], Niemi, J.V.[5], and Petäjä, T.[1]

[1]Institute of Atmospheric and Earth System Science / Physics, Faculty of Science, University of Helsinki, Finland

[2]Finnish Meteorological Institute, Helsinki, Finland

[3]Pegasor Oy, Finland

[4]Vaisala Oy, Finland

[5]Helsinki Region Environmental Services Authority (HSY), Finland

30/04/2018

Table of Contents

1. Introduction

Air quality (AQ) is one of the grand challenges that the society faces at the moment. The problem arises from anthropogenic emissions of pollution gases and particulate matter. Furthermore, the air quality deteriorates via atmospheric chemical reactions producing harmful gas phase pollutants (ozone) and secondary particulate matter, typically enhanced by photochemical reactions. Meteorology governs the dispersion of pollutants, both vertically and horizontally.

Traditionally, the air quality in the urban environment is monitored with a network of stations providing in-situ observations of key gas phase pollutants (O_3, NO_x, SO_2) and particulate mass concentration below 2.5 µm or 10 µm i.e. $PM_{2.5}$ and PM_{10}, respectively. The regulatory network is constructed to represent different urban environments (kerbside, urban background, rural) and the air quality conditions at these sites are reported and taken to be as representatives for similar urban environments.

Recently, this traditional view has been improved by implementing more numerous supplementary air quality observations (e.g. Moltchanov et al. 2015) by combining this dense observation network with more comprehensive benchmarking supersites and existing in-situ air quality network data (Borrego et al. 2016). The supplementary equipment provides spatial variability with a coarse capacity that require further development (Castell et al. 2017). The product is envisioned to be an integrated view on the air quality situation, which is further elaborated with synthesis with a model prediction providing a spatially and temporally high-resolution picture of air quality in the urban area.

In Helsinki region, the observations from two supersites – one representing urban background (SMEAR III station in Kumpula, Järvi et al. 2009) and the other an urban street canyon (Mäkelänkatu observation site, Kaski et al., 2017) – and an authority network are extended with supplementary observations with Vaisala AQT420 sensors, which detect the traditional gaseous and particulate AQ parameters. The observations are integrated with a fusion modelling framework (FMI-ENFUSER, Karppinen and Johansson, 2018) to provide spatially representative air pollution fields that take into account in-situ observations, spatio-temporal variability of pollution sources (e.g. traffic, industry) and meteorological situation.

The supersites and some of the authority network sites include also observations of additional parameters that are relevant for AQ situational awareness. These parameters include aerosol particle number concentration (N), black carbon concentration (BC), lung deposited surface area (LDSA), and on-line chemical composition of atmospheric aerosol particles. The supersite observations also provide data on targeted trace gases, such as sulfuric acid. These comprehensive observations can be used to derive proxy variables from the standard air quality observations to expand the suite of parameters potentially connected to negative health effects of air pollution.

In this report, we describe the benefit of observing the new AQ parameters. Since instruments for detecting the concentrations of most of these parameters are expensive, for several of them we derive proxies, with which their values can be estimated in better spatial resolution with the full authority network or even with the denser AQT420-network.

2. Recommendations for new AQ observations

We identify in the section below few targeted new observables that are pertinent to air quality particularly in the urban environment. The new observations are either to be implemented into supersite observation sites or as independent small instruments that provide information with high spatial and temporal resolution.

As a brief summary, Table 1 provides a list of currently regulated and unregulated AQ parameters with their main sources in the urban environment with corresponding key activities that can improve the air quality.

Table 1. Currently regulated and unregulated air quality (AQ) parameters for continuous monitoring of particulate pollutants in urban air. The unregulated parameters (BC, LDSA, N) are all indicators of local combustion emissions in urban areas. However, the concentrations of these parameters reflect and emphasize partly different combustion sources. For instance, residential wood combustion vs. traffic exhausts are emphasized in the following order; BC > LDSA > N. In other words, residential wood combustion has a significant impact on BC concentrations but only a minor impact on PN concentration. Particles from local traffic exhaust emissions have dominant impact on urban PN concentrations.

AQ parameter	**Typical main sources of particles in urban and suburban areas in the Helsinki metropolitan area**	**Parameter focuses local air protection measures**
Coarse thoracic particle mass ($PM_{2.5\text{-}10}$)	• Street dust (asphalt wear, sanding materials, soil dust, tyre and break wear…) • Dust from construction sites	Street cleaning, dust binding, sieved sanding materials, non-studded winter tyres…
Fine particle mass ($PM_{2.5}$)	• Regionally and long-range transported particles • Local emissions from ○ vehicle exhausts ○ street dust ○ residential wood combustion	Traffic exhausts (old vehicles), street dust and residential wood combustion
Black carbon (BC)	• Local emissions from ○ residential wood combustion ○ diesel vehicles without particulate filter • Regionally and long-range transported particles	Residential wood combustion and old diesel vehicles
Lung deposited surface area (LDSA)	• Local emissions from ○ traffic exhausts ○ residential wood combustion • Regionally and long-range transported particles	Traffic exhausts (old vehicles) and residential wood combustion
Particle number (N)	• Local emission from traffic exhausts • Regionally and long-range transported particles and new particle formation in the atmosphere (nucleation)	Traffic exhausts

2.1 Direct observations of new AQ parameters

2.1.1 Particle number concentrations with small sensors

Aerosol number concentration is relevant for assessing aerosol health and climate effects. The studies show that aerosol number exposure causes negative health effects (e.g. von Klot et al. 2005). In an urban environment, aerosol number is dominated by the particles in the ultra-fine size range, below 50 nm in diameter (e.g. von Bismarck-Osten et al. 2013) and the number concentration varies very rapidly in temporal scales of minutes and spatial scales of tens of meters (e.g. Dos Santos-Juusela et al. 2013, Kukkonen et al. 2016).

The ultra-fine particles are typically observed with Condensation Particle Counters (CPC, McMurry, 2000), where the particles are first exposed to supersaturated vapor, which condenses onto the particles making them large enough to be detected optically. Automotive industry is regulated in terms of aerosol number emission with smallest detectable particle size of 23 nm (EURO 5 and EURO 6), as during operation, combustion engine produces a significant number of ultra-fine aerosol particles. This is mitigated by filtering the exhaust gases.

The CPCs are typically expensive, table-top research instruments that can be operated in well-facilitated air quality observation sites. However, recently we have developed a small-size CPC that can operate autonomously for extended periods (Wu et al. 2019 in preparation). This opens up new opportunities to expand the aerosol number concentration measurement networks to capture the rapidly changing number concentrations in the urban environment. This can provide new insights into personalized ultra-fine aerosol exposure analysis.

2.1.2 Black carbon concentration

Black carbon (BC) is strongly light-absorbing carbonaceous material that is emitted in the atmosphere as fine particles as a side product of incomplete combustion. It has been shown that combustion-derived particles are more relevant to the human health than aerosol particles from other sources (Janssen et al., 2011). Since BC is an indicator of combustion related aerosol particles, it gives additional information about the health effects of $PM_{2.5}$, marking the importance of monitoring BC in addition to $PM_{2.5}$.

In the Helsinki region, the concentration of BC is measured by an Aethalometer (Magee Scientific model AE-31) and a Multi Angle Absorption Photometer (MAAP, Thermo Scientific model 5012). These online instruments collect the aerosol particles on a filter medium and measure the light transmittance through the aerosol-laden filter. The concentration of BC is derived from the change of the light transmittance, which decreases over time when the filter gets more loaded with absorbing aerosol particles. Aethalometer measures the BC concentration on seven wavelengths ranging from near UV (370 nm) to near infrared (950 nm) and MAAP measures the BC concentration only at red wavelength (637 nm). In addition to the supersites (SMEAR III and Mäkelänkatu), the concentration of BC is monitored in different types locations around the Helsinki metropolitan area covering traffic sites, detached housing areas and background sites.

In the Helsinki metropolitan area, BC makes about 5 – 20 % of the total $PM_{2.5}$, with the highest fractions occurring at the traffic sites and lowest fraction occurring at regional background. BC concentration has a more pronounced spatial and temporal variation than $PM_{2.5}$, since the sources of BC are heavily related to human activities and because it does not have as strong background as $PM_{2.5}$ has. Since the main sources of BC in the Helsinki region are traffic and wood burning (Helin et al., 2018), we can see clear diurnal and weekly cycles in the BC concentration at the traffic sites and detached house areas. During weekdays at traffic sites, the BC concentration increases with the morning rush hour starts and it starts to decrease in the noon when the boundary layer is being mixed. Due to the mixing, the concentration does not increase as high during the afternoon rush hour as in the morning. During weekends, the BC concentration does not increase as much as during weekdays due to less traffic. The weekly and diurnal cycles are different at the detached house areas. During weekdays at the housing areas, the BC concentration is higher during evening than during the morning rush hour. The evening concentration peak is even more pronounced during the weekend and especially during the cold season. The elevated evening BC concentration are caused by heating of the houses and saunas by burning wood.

2.1.3 Lung deposited surface area

Epidemiological studies have shown strong correlation between mass-based PM exposure (i.e. $PM_{2.5}$) and premature mortality, but the detailed processes governing the harmful health effects are still not fully understood. As a consequent, it has been hypothesized that surface related chemistry of particles may be a significant factor when assessing the harmfulness of PM. Toxic chemicals are attached to the surfaces of particles and transported to the deepest parts of human respiratory system via the particles. The surface area, and a so-called lung deposited surface area (LDSA) in particular, is therefore a parameter of interest. LDSA describes the computational surface area of particles depositing to the deepest parts (i.e. alveolar region) of human respiratory system and thus takes into account the potential of particle surface related chemistry.

LDSA concentrations are mainly driven by small (< 400 nm) particles as the alveolar deposition fraction of particles of this size is high, and they are typically present in high numbers, especially in urban areas. Anthropogenic sources such as vehicular exhaust emissions and residential wood combustion are typical sources of high LDSA concentrations as particles emitted from these sources are often in the ultrafine size range. Due to the small size of particles LDSA concentrations cannot be measured with optical methods.

Concentrations of LDSA are typically measured with a so-called diffusion charging-based technique where particles are charged using a unipolar corona charger. Formed ions are driven onto the surfaces of particles by diffusional forces, and a current signal, which is proportional to the number of ions attached to the surfaces of particles, can be measured by collecting the particles with a Faraday cup electrometer or by using a measurement of escaping current. This method enables measurement of ultrafine particles and, more specifically, the LDSA concentration with good accuracy and high temporal resolution (1 Hz). Currently, several different instruments are available on the markets which utilize the aforesaid technique as their operation principle.

2.1.4 On-line aerosol chemical composition

Ambient aerosol particles comprise of a mixture of substances originating from a variety of diverse activities, including fuel combustion (from vehicles, power generation, and industrial facilities), biomass burning (forest fires, agricultural burning, heating) and industrial processes. In addition to this, a large number of biogenic sources, e.g. sea spray, volcanic emissions, windblown soil, influence aerosol concentrations. Primary particles are directly introduced into the atmosphere, whereas the secondary aerosol particles are formed in atmosphere from gaseous compounds. The major constituents of atmospheric aerosol particles are inorganic ions, carbonaceous compounds, trace metals and particle-bound water. The composition is mostly depending on the source, but it is also affected by the physico-chemical processes like aging in the atmosphere and aerosol removal processes. Processes in the atmosphere are rapid and traditional PM-filter collections with long collection times do not provide an adequate picture of the constantly-evolving situation Due to the variety of sources and dynamics of multiphase aerosol system, the online measurements with high-time resolution are needed to accurately describe the temporal variation of aerosol composition and sources. The new online analyzing methods, such as aerosol mass spectrometers are needed to the temporal variation of aerosol composition and sources.

Aerosol mass spectrometers have been developed to measure the composition of submicron aerosol particles in real time. Aerosol mass spectrometers consist of an aerodynamic lens to form particle beam, vacuum chamber with vaporizer and ionizer and a either quadruple or time-of-flight mass spectrometer detector (Jayne, 2000; Ng et al., 2011; Onasch et al., 2012). Several different aerosol mass spectrometers have been developed depending of the need of the user; Aerosol mass spectrometer (AMS) with added laser vaporizer can analyzer the full size resolved chemical composition including organics, inorganic ions (sulfate, nitrate, ammonium, chloride), black carbon and metals, whereas Aerosol Chemical Speciation monitors (ACSM) are unit-mass resolution instruments that can measure the composition of non-refractive PM i.e. organics and inorganic ions.

Aerosol mass spectrometers combined with statistical Positive Matrix Factorization (PMF) source apportionment have provided important information about the sources of PM in Helsinki area. The main sources in Helsinki area are traffic, biomass burning, secondary aerosol formation and Long-range transport (Carbone et al., 2014; Timonen et al., 2013; Aurela et al., 2015). Observed aerosol composition depends on prevailing PM sources. In the urban environment the aerosol composition is typically dominated by organics (40-60% of submicron PM), BC (5-20%) and smaller amounts of inorganic (5-30%) ions are observed (Teinilä et al., 2019, Aurela et al., 2015). In long-range transported air masses, the contribution of inorganic ions, especially sulfate can be higher (Saarikoski et al., 2007; Saarikoski et al., 2008).

2.1.5 Aerosol precursor gases, such as sulfuric acid and extremely low volatile organic vapors

Modern atmospheric mass spectrometry has developed techniques that are sensitive enough to detect gas-phase precursor vapors on-line directly from the atmosphere with ppq-sensitivity (e.g. Petäjä et al. 2009, Junninen et al. 2010, Sipilä et al .2016). One specific instrument with relevance to air quality is Chemical Ionization – Atmospheric Pressure interface Time-of-Flight mass spectrometer (CI-APiTOF, Jokinen et al. 2012), which provides quantitative concentrations of gas-phase sulfuric acid and data on other aerosol precursor vapours, such as extremely low-volatile oxidized organics (Ehn et al. 2014).

Operating these research-grade instruments as part of supersite network in urban environment will provide new insights into secondary air pollution (e.g. Kulmala et al. 2014, Kulmala et al. 2016). This data can be utilized to develop a suite of proxy variables describing e.g. the spatial variability of gas-phase sulfuric acid in the urban environment, when combined with affordable instruments providing sulphur dioxide measurements and solar radiation. Furthermore, this data can be used to assess e.g. atmospheric oxidative potential and / or deterioration of urban surfaces due to acid deposition (Saffari et al. 2015, Castillo-Miranda et al. 2017)

2.2 Proxies for the new AQ parameters

The currently deployed instruments for measuring the new AQ parameters, described in Sect 2.1, are too expensive for distributing them to a dense network within an urban area. In this section, we describe proxies that can be applied for improving the spatial representation of the new AQ parameters. The proxies are based on the variables measured at the Helsinki authority network stations and with the AQT420 sensors. In other words, we derive equations that express the new AQ parameters as functions of the traditional gaseous and particulate AQ parameters. With this information, the new AQ parameters can be implemented to the modelling framework with similar resolutions than the traditional parameters.

The method applied for determining the proxies is similar to the method described in Paasonen et al. (2010) and Kontkanen et al. (2016). The proxies are determined by first parameterising the principal component (the variable with which the target variable shows the highest correlation) and then determining on which other variables the bias of this first parameterisation depends. This is illustrated in Sect. 2.1.1, where the proxy for total particle number concentration N (as a target variable) is determined.

The proxies presented in this work are derived with the data gathered at SMEAR III station, except for BC proxy, which is derived with data from SMEAR III, Mäkelänkatu supersite and authority network station in Itä-Hakkila.

2.2.1 Particle number concentration proxies

The particle number concentration in diameter range 3-1000 nm (*N*) was calculated from the particle number size distribution data, recorded with DMPS (Differential mobility particle sizer; Aalto et al., 2001). The principal component, out of those recordable with the AQT420 sensor, with which *N* was observed to correlate was nitrogen dioxide concentration ($[\mathrm{NO_2}]$; Fig 1a). This is reasonable, since the main source of both ultrafine particles and $\mathrm{NO_2}$ in the urban environment is road traffic. The particle concentration *N* seemed to be dependent also on RH, based on the colouring of Fig 1a. This was confirmed by depicting the ratio of the observed *N* and the first proxy $f([\mathrm{NO_2}])$ (determined from the linear least squares fit in $\log_{10}(N)$ vs $\log_{10}([\mathrm{NO_2}])$) as a function of relative humidity (Fig. 1b). The log to linear least squares fitting to this figure resulted in the second parameter f(RH). The log-log and log-linear dependencies of *N* on [NO2] and RH, respectively, suggest that the proxy is of form

$$N = a \times [\mathrm{NO_2}]^{s_1} \times 10^{s_2 \times \mathrm{RH}}, \qquad (1)$$

where s_1 and s_2 are the slopes of the fits in Fig 1a and Fig 1b, respectively, and $a = 10^{I_1 \times I_2}$, where I_1 and I_2 are the intercepts of the fits in Fig 1a and Fig 1b, respectively.

Finally, the factors s_1, s_2 and *a* were optimized to produce the smallest possible ratio $V_{90/10}$ between the 90th and 10th percentiles of data point specific measurement/proxy -ratios. This method drives the proxy towards 1:1 line with respect to the target variable (Paasonen et al., 2010; Kontkanen et al., 2016). The proxy with optimized values for particle number concentration was

$$N = 3470 \times [\mathrm{NO_2}]^{0,60} \times 10^{-0.0034 \times \mathrm{RH}}.$$

It is important to notice that this proxy is not derived directly from the physical formation and losses of particles. Thus, the proxy cannot be directly applied to describe N in different environments, representing different types of particle sources, but proxies for different environments should be derived.

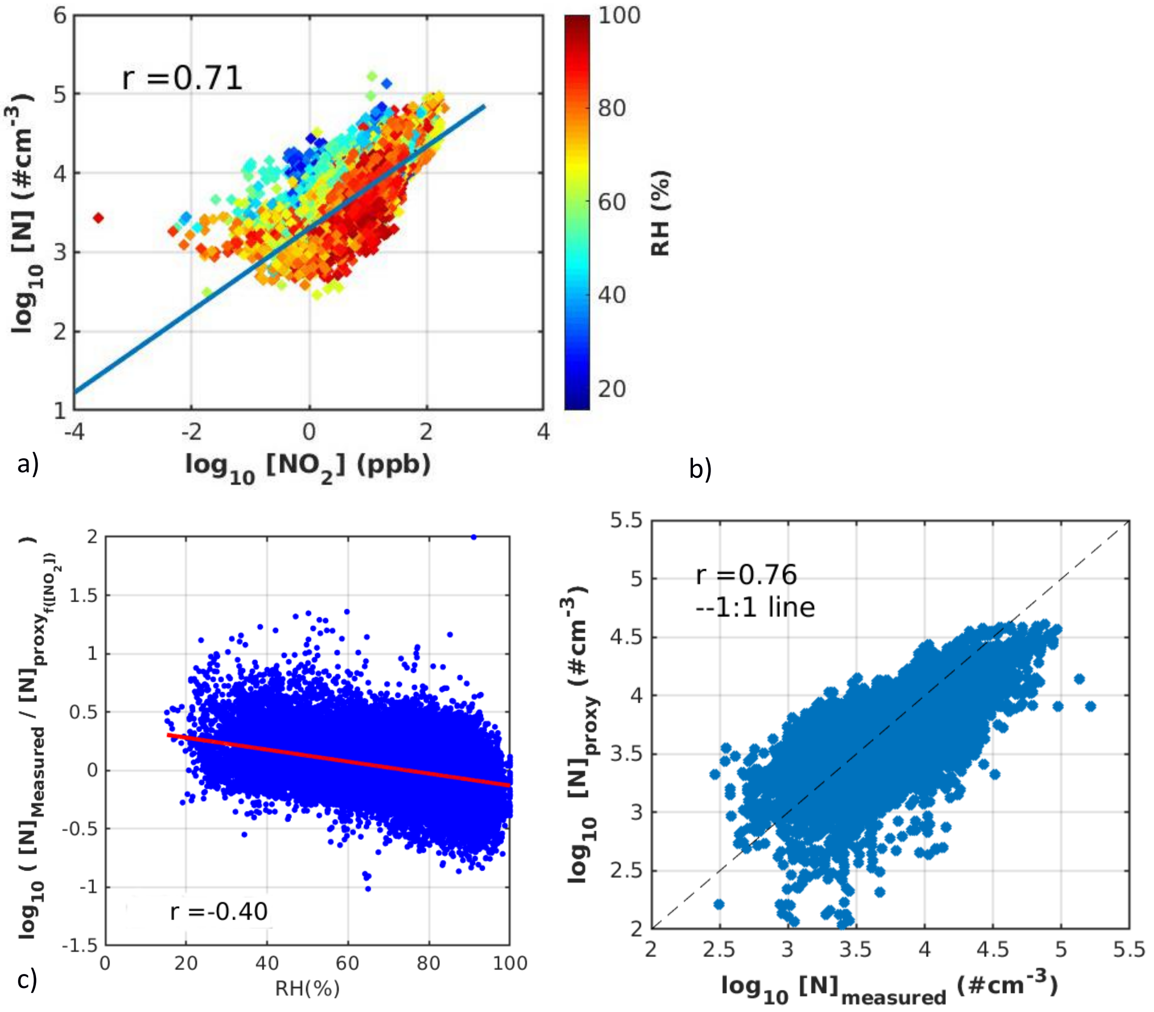

Figure 1. Derivation of proxy for particle number concentration (N). Linear least squares fittings in panels a) and b) are the starting points for the optimization of the constants in Eq. (1). See text for more details.

2.2.2 Black carbon concentration proxies

The proxy for black carbon mass concentration (BC) was determined in a similar manner to the particle number concentration proxy. We applied three different BC observation data sets to derive the proxy – one in street canyon in Mäkelänkatu supersite, one in Kumpula SMEAR III urban background site, and one in Itä-Hakkila residential single-house area. For all the sites, the principal variables for the proxies were $PM_{2.5}$ and NO_2 concentrations in a power law form, i.e. the proxy took the form

$$[\mathrm{BC}] = a \times [\mathrm{PM}_{2.5}]^{s_1} \times [\mathrm{NO}_2]^{s_1}, \qquad (2)$$

Figure 2 shows the derivation of the proxy for the combined data set, where all the three above mentioned sites are included. The values determined for the coefficients in Eq. (2) with the separate and combined data sets are presented in Table 2. The slope values are surprisingly similar at very different environments, such as Itä-Hakkila, where the main source of BC is the residential wood combustion, and Mäkelänkatu, where the main source of BC is the traffic.

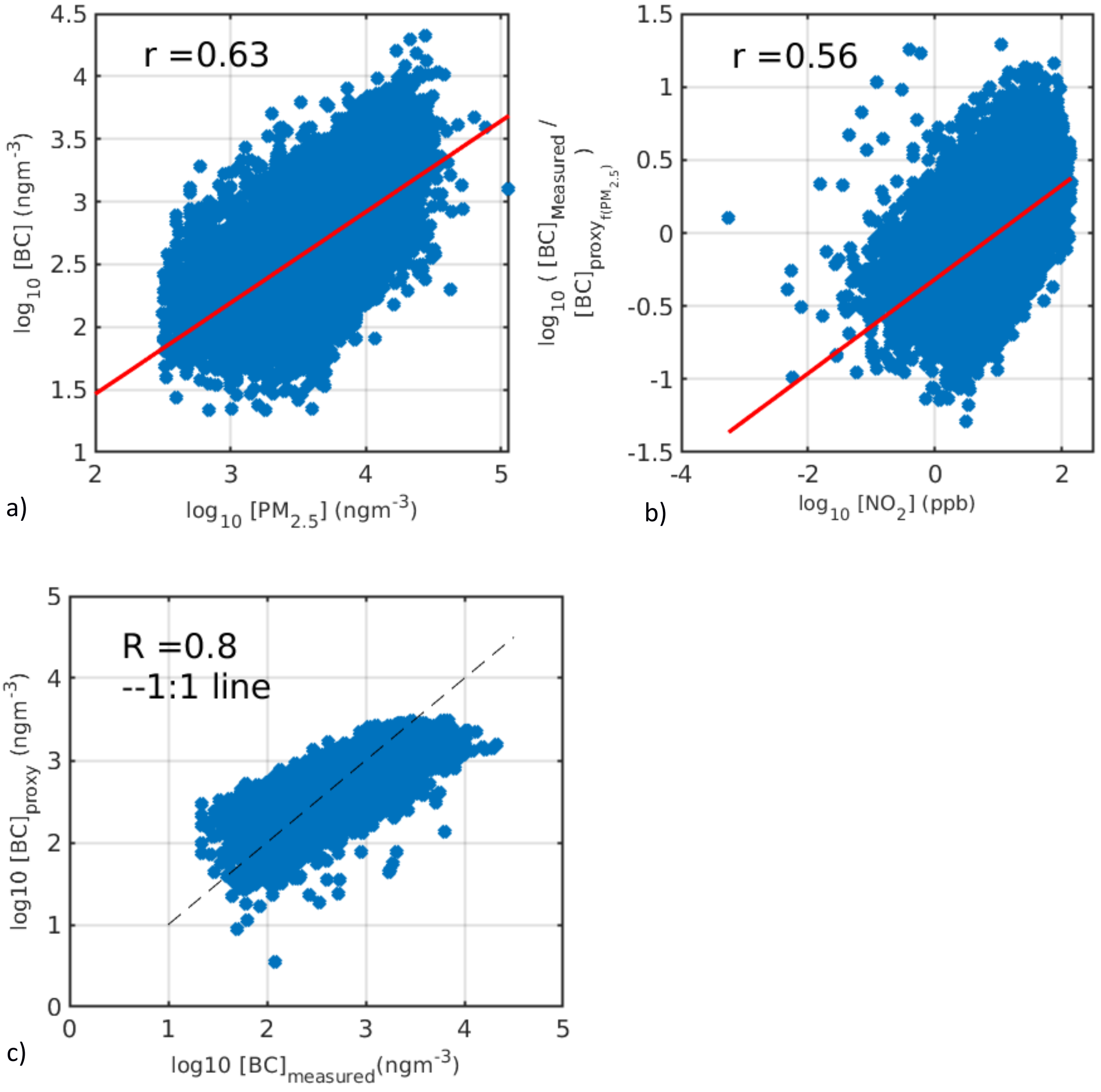

Figure 2. Derivation of the proxy for BC mass concentration, determined with a combined data set from Mäkelänkatu, Itä-Hakkila and Kumpula sites.

Table 2. Parameters defined for BC-proxy (Eq. 2) from the combined and separate BC observation data sets. $V_{90/10}$ describes the ratio of 90th and 10th percentile of data point-specific measurement/proxy ratios, and r is the Pearson's correlation coefficient.

Data set	**Constant (*a*)**	**Slope (s_1)**	**Slope (s_2)**	**$V_{90/10}$**	***r***
Combined	5.70	0.42	0.41	3.67	0.80
Mäkelänkatu	1.69	0.41	0.78	2.59	0.89
Itä-Hakkila	2.81	0.44	0.63	3.99	0.77
Kumpula	10.73	0.36	0.43	3.30	0.81

2.2.3 Lung deposited surface area proxies

Lung deposited surface area (LDSA) of the aerosol particles in urban environment is typically strongly dependent on the traffic emissions (Kuula et al. 2018). This is because the particles with diameters of ten or tens of nanometres are transported much more efficiently to lungs than those with diameters close to or over 100 nm (e.g. Alföldy et al., 2009), and the traffic emissions play an important role on the concentration of particles in this size range. Thus, it is reasonable that the strongest correlations against LDSA out of the pollutants observed with AQT420 were found for NO_2 (see Sect. 2.2.1). Other components observed to be related to LDSA concentration, in addition to NO2, were PM2.5, RH and temperature (Figure 3). We also determined whether the proxy could be improved by taking into account the observed particle number concentrations. We applied as total particle number concentration (N) the concentration of particles with diameters larger than 10 nm, calculated from the DMPS data (see Sect. 2.2.1). Indeed, all the correlations between the observed LDSA and the variables applied for the proxy increased, when the NO_2 was replaced with N (Figure 4). The efficacy of the final proxy was also better when N was applied instead of NO_2 (Figure 5), and the final optimized proxies with these variables were

$$\mathrm{LDSA}_{\mathrm{AQT\ proxy}} = 0.97 \times 10^{-4} \times [\mathrm{NO_2}]^{0{,}44} \times [\mathrm{PM_{2.5}}]^{0{,}22} \times 10^{-0.0010\times\mathrm{RH}} \times 10^{0.0044\times\mathrm{T}}$$

and

$$\mathrm{LDSA}_{\mathrm{AQT+N\ proxy}} = 1.36 \times 10^{-4} \times \mathrm{N}^{0{,}70} \times [\mathrm{PM_{2.5}}]^{0{,}33} \times 10^{0.0084\times\mathrm{T}} \times 10^{0.0021\times\mathrm{RH}}.$$

The unit of LDSA in these proxies is pA, referring to the electric signal within the instrument. Calibration coefficient, determined elsewhere, should be applied for determining the real LDSA values. These proxies were derived from only four months data (Feb 2018 – May 2018), because only during that period both LDSA and $PM_{2.5}$ data were available.

It is notable that, even though the correlation coefficient between the (logarithmic values of) observed and the proxy making use of N (r=0.89, Fig 5b) is not drastically different than the one with only AQT determined pollutant and meteorological variables (r=0.85, Fig 5a), the proxy utilizing N_{tot} captures clearly better the high values of LDSA.

It is also important to note that the LDSA proxy is not derived directly from the physical formation and losses of particles contributing to LDSA. Thus, the proxy should be determined in different environment within the urban area. This was not done within the HAQT project, but remains a task for future projects.

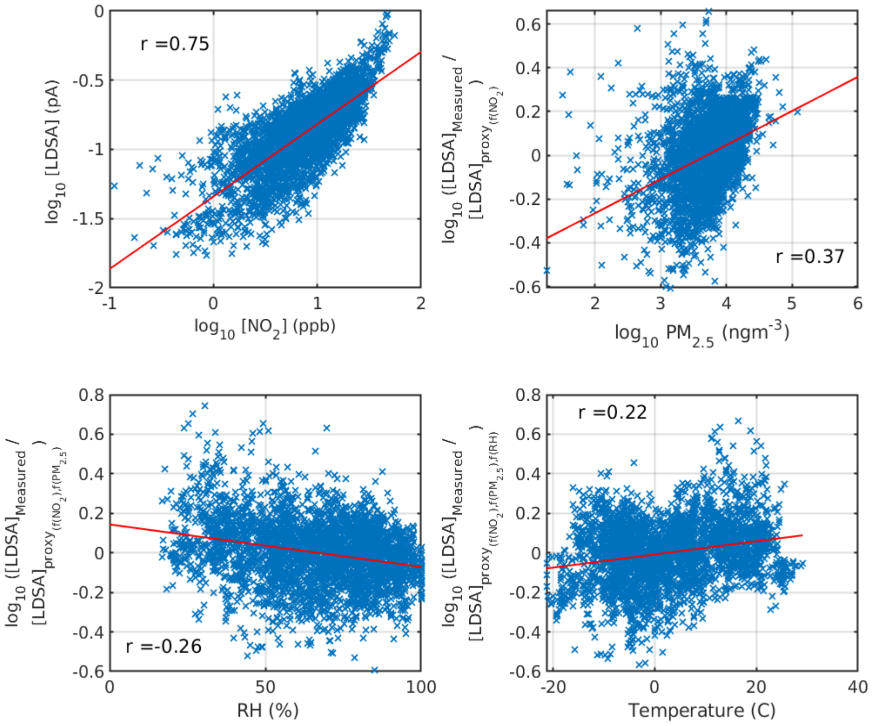

Figure 3. Derivation of a LDSA proxy from the pollutants and meteorological variables detected with AQT420. The unit of LDSA is pA, referring to the electric signal within the instrument.

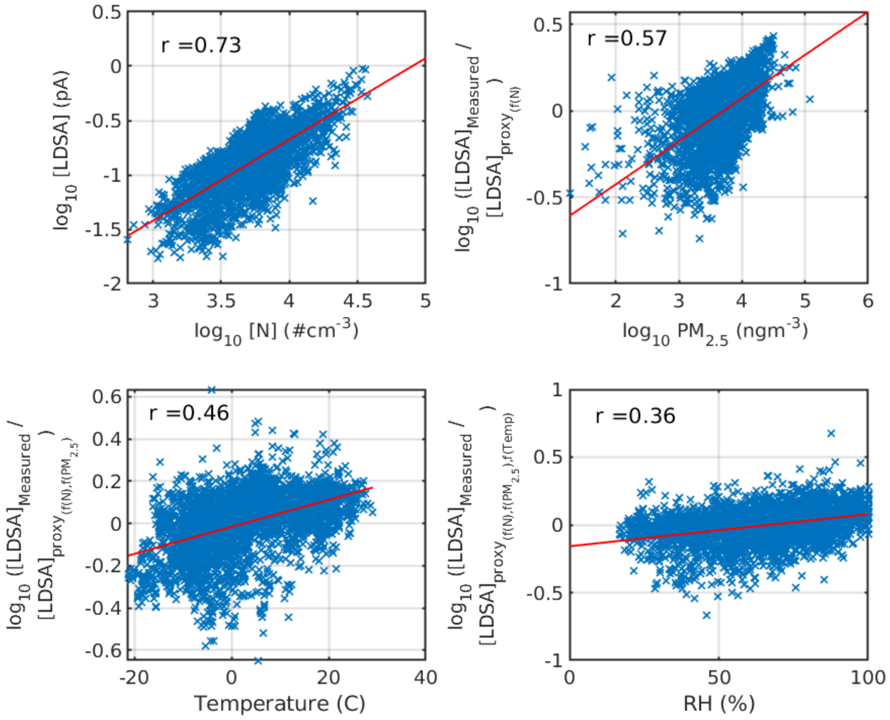

Figure 4. Derivation of a LDSA proxy from the pollutants and meteorological variables detected with AQT420, accompanied with number concentration of particles with diameters larger than 10 nm (N). The unit of LDSA is pA, referring to the electric signal within the instrument.

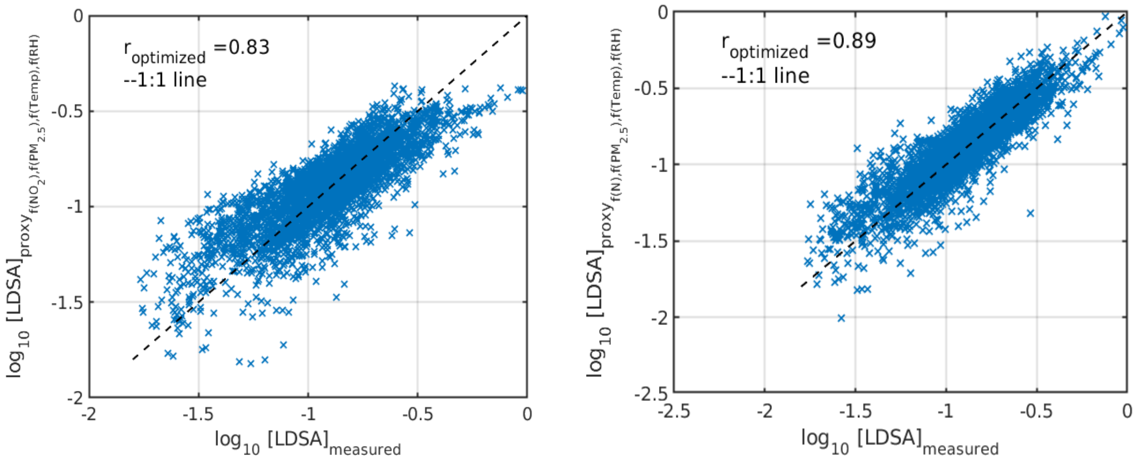

Figure 5. Performance of the optimized proxies when only AQT variables are applied (left) and when AQT variables are complemented with particle number concentration (right).

2.2.4 Condensation sink proxies

The derivation of the proxy for condensations sink, representing the probability of vapour molecules to collide with the total aerosol surface area, is depicted in Figure 6. The proxy was derived from half a year of data, from 1.2. to 31.7.2018. There were clear minimum values for $PM_{2.5}$ and NO_2, under which these variables did not correlate with CS, namely $PM_{2.5} = 10^{3.2}$ ngm^{-3} and $NO_2 = 10^{-0.1}$ ppb. Thus, for the derivation of the parameters above, we limited these variables by generating concentration vectors $[PM_{2.5}']=[PM_{2.5}]$ and setting $[PM_{2.5}'] = 10^{3.2}$ ngm^{-3} for the times when $[PM_{2.5}]<10^{3.2}$ ngm^{-3}, and $[NO_2']=[NO_2]$ and setting $[NO_2'] = 10^{-0.1}$ ppb for the times when $[NO_2]<10^{-0.1}$ ppb. The CS proxy took the form

$$\mathrm{CS} = a \times [\mathrm{PM}_{2.5}']^{s_1} \times [\mathrm{NO}_2']^{s_1} \times 10^{s_3 \times \mathrm{RH}} \times 10^{s_4 \times \mathrm{T}}, \qquad (3)$$

and with the optimized parameter values Eq. (3) becomes

$$\mathrm{CS} = 2.98 \times 10^{-5} \times [\mathrm{PM}_{2.5}']^{0.44} \times [\mathrm{NO}_2']^{0.29} \times 10^{-0.005 \times \mathrm{RH}} \times 10^{-0.011 \times \mathrm{T}}.$$

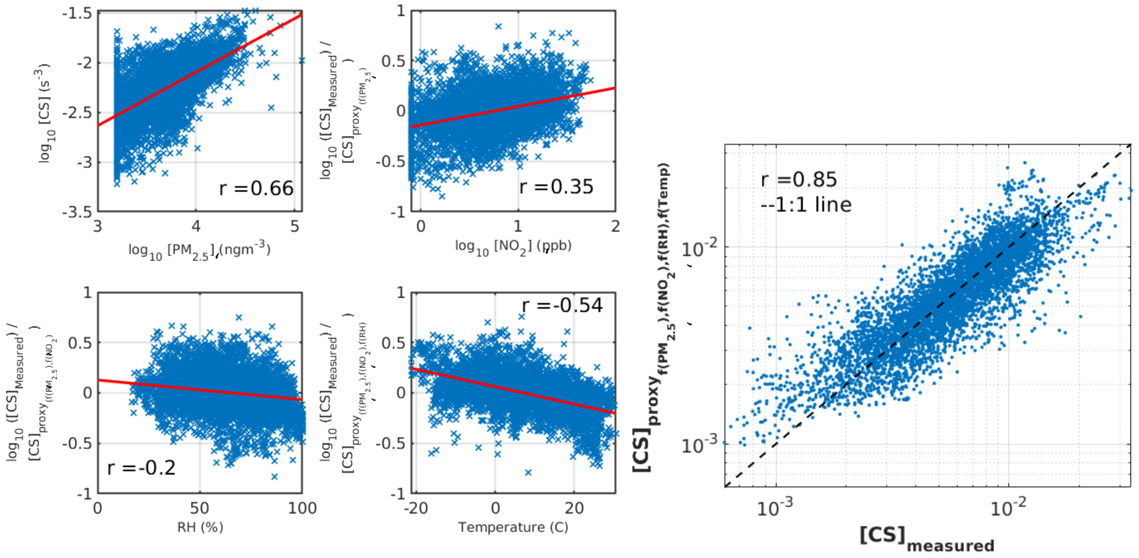

Figure 6. Derivation (four panels on left hand side) of the condensation sink proxy, and the comparison of the proxy with observed CS (right hand side).

2.2.5 Sulfuric acid concentration proxies

The derivation of the proxy for sulphuric acid concentration ([SA]) is described in Figure 4. The sulphuric acid measurements were conducted at SMEAR III only for a month, from 3.5. to 4.6.2018. By progressing in a similar manner than for the other variables above, the optimized proxy takes the form

$$[\mathrm{SA}] = \frac{1.27\times10^4\times[\mathrm{SO_2}]^{1.39}\times\mathrm{GlobRad}^{0.67}}{\mathrm{CS}_{proxy}^{0.30}}\,10^{-0.0029\times\mathrm{RH}},$$

where GlobRad stands for global radiation, measured in [W/m^2]. Unlike the proxies in the previous sections, the form of this sulphuric acid proxy is close to the pseudo-steady-state assumption, which is expressed as the ratio of sources and sinks of the studied compound. The formation rate of sulphuric acid is determined by the reaction rate between SO_2 and OH radical and OH concentration can be estimated with the level of global radiation (GlobRad) (Petäjä et al., 2009). The main sink for sulphuric acid is CS, which is typically slightly enhanced by increasing RH (Mikkonen et al., 2011). The derived proxy is in good agreement with the previous proxies generated with different methods (Petäjä et al., 2009; Mikkonen et al., 2011).

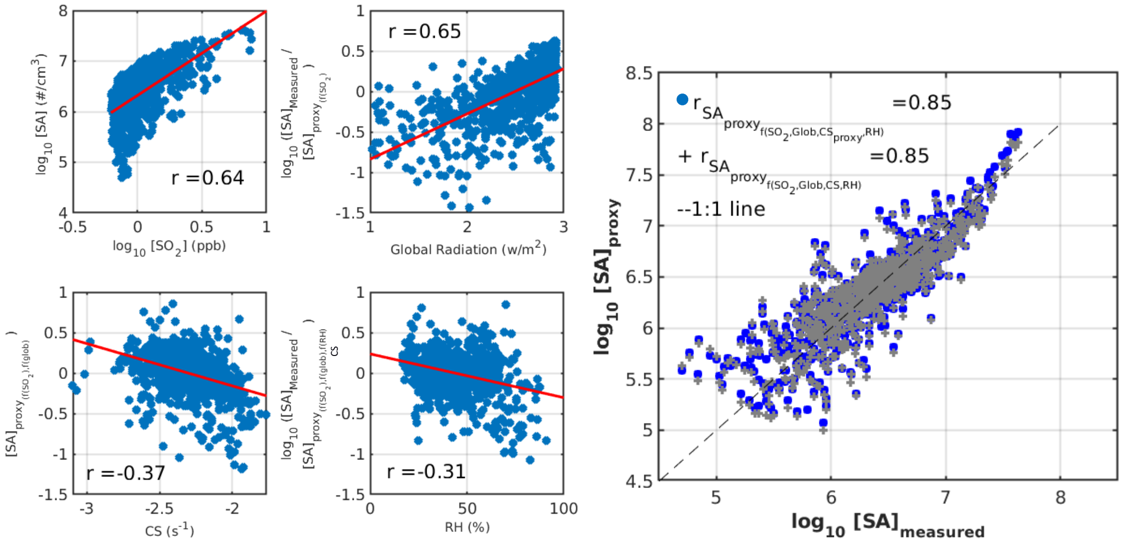

Figure 7. Derivation (four panels on left hand side) of the sulphuric acid proxy, and the comparison of the proxy with observed SA concentration (right hand side), where blue points are received with the CS proxy and the grey crosses with observed CS.

3. Summary

In this deliverable we discuss variables, additional to the traditional air pollutants, that are relevant for assessing in terms of air quality. In specific, the variables discussed in this deliverable are aerosol particle number concentration (N), black carbon concentration (BC), lung deposited surface are (LDSA), sulphuric acid concentration (SA) and concentration of extremely low volatile organic vapour concentrations. Out of these parameters, BC and LDSA are directly linked to human health. N is a parameter strongly linked to LDSA, since the highest number concentrations are typically encountered in size ranges, which deposit efficiently in the human lungs. SA and low volatile organic vapours are related to aerosol formation, both in terms of particle number and mass.

We derive proxies, based on the data from SMEAR III supersite, for N, BC, LDSA and SA, as well as for condensation sink (CS) which is a parameter needed for SA proxy and possible other vapour proxies to be derived in future. All proxies showed reasonable correlations with the observations, the weakest correlation being for N (r=0.76) and the strongest, achieved with the parameters measurable with AQT420 only, for SA and CS (r=0.85). The correlation coefficient between the measured and proxy LDSA increased from r=0.83, achieved with variables measurable with AQT420, to r=0.89, when also the observed N was utilized for generating the proxy. Out of the proxies described in this deliverable, only the proxy for particle number concentration (N) is based on several years of data. The proxy for condensation sink (CS) is based on half a year of data, LDSA on four months and SA only on one month of data. Thus, the constants in the proxies need to be re-evaluated when longer data sets of the required parameters are available.

The proxies generated in this work can be applied when estimating the spatial distribution of the new AQ parameters. We determined the BC proxy for three different environments – street canyon, urban background and small house area sites. The proxies optimized for these environments were mainly similar, even though the different proxy components, NO_2 related to traffic and $PM_{2.5}$ to residential wood combustion, were weighted slightly differently. The proxy determined from a combined data set of these different environments represented relatively well all the environments.

It is notable that the proxy for LDSA is also expected to be different in different types of urban environments. Since in this study the LDSA proxy was derived only at SMEAR III, it should be investigated in the future in different environments, e.g. small house area and street canyon site.

References

Aalto, P., Hämeri, K., Becker, E., Weber, R., Salm, J., Mäkelä, J., Hoell, C., O'Dowd, C. D., Karlson, H., Hansson, H.-C., Väkevä, M., Koponen, I. K., Buzorius, G., and Kulmala, M. (2001): Physical characterization of aerosol particles during nucleation events, Tellus B, 53, 344–358.

Alföldy, B., Giechaskiel, B., Hofmann, W., and Drossinos, Y. (2009): Size distribution dependent lung deposition of diesel exhaust particles, J. Aerosol Sci., 40, 652.

Aurela, M., Saarikoski, S., Niemi, J. V., Canonaco, F., Prevot, A. S. H., Frey, A., Carbone, S., Kousa, A., and Hillamo, R. (2015): Chemical and source characterization of submicron particles at residential and traffic sites in the Helsinki Metropolitan Area, Finland, Aerosol and Air Quality Research, 15, 1213-1226, 10.4209/aaqr.2014.11.0279.

Borrego, C., Costa, A.M., Ginja, J., Amorim, M., Coutinho, M., Karatzas, K., Sioumis, T., Katsifar, N., Konstantinidis, K., De Vito, S., Esposito, E., Smith, P., Gérard, A.P., Francis, A., Castell, N., Schneider, P., Viana, M., Minguillón, M.C.M., Reimringer, W., Otjes, R.P., von Sicard, O., Pohle, R., Elen, B., Suriano, D., Pfistern, V., Prato, M., Dipinto, S. and Penza M. (2016): Assessment of air quality microsensors versus reference methods: The EuNetAir joint exercise, Atmos. Environ. 147, 246-263.

Carbone, S., Aurela, M., Saarnio, K., Saarikoski, S., Timonen, H., Frey, A., Sueper, D., Ulbrich, I. M., Jimenez, J. L., Kulmala, M., Worsnop, D. R., and Hillamo, R. E. (2014): Wintertime Aerosol Chemistry in Sub-Arctic Urban Air, Aerosol Science and Technology, 48, 313-323, 10.1080/02786826.2013.875115.

Castell, N., Dauge, F.R., Schneider, P., Vogt, M., Lerner, U., Fishbain, B., Broday, D. and Bartonova, A. (2017): Can commercial low-cost sensor platforms contribute to air qualitymonitoring and exposure estimates? Environ. Internat. 99, 293-302.

Castillo-Miranda, J.O., Torres-Jardón, R., Garcia-Reynoso, J.A., Mar-Morales, B.E., Rodriguez-Gómez, F.J., Ruiz-Ruárez, L.G. (2017): Mapping recession risk for cultural heritage stone in Mexico City due to dry and wet deposition of urban air pollutants, Atmósfera 30, http://dx.doi.org/10.20937/atm.2017.30.03.01

Dos Santos-Juusela, V., Petäjä, T., Kousa, A. and Hämeri, K. (2013): Spatial - temporal variations of particle number concentrations between a busy street and the urban background, Atmos. Environ. 79, 324-333.

Ehn, M., Thornton, J.A., Kleist, E., Sipilä, M., Junninen, H., Pullinen, I., Springer, M., Rubach, F., Tillmann, R., Lee, B., Lopez-Hilfiker, F., Andres, S., Acir, I.-H., Rissanen, M., Jokinen, T., Schobesberger, S., Kontkanen, J., Nieminen, T., Kurtén, T., Nielsen, L.B., Jørgensen, S., Kjaergaard, H.G., Canagaratna, M., Dal Maso, M., Berndt, T., Petäjä, T., Wahner, A., Kerminen, V.-M., Kulmala, M., Worsnop, D.R., Wildt, J. and Mentel, T.F. (2014): A large source of low-volatility secondary organic aerosol, Nature 506, 476–479.

Euro 5/6 standards (2009/2014): Regulation 715/2007

Jayne, J. T., Leard, D.C., Zhang, X., Davidovits, P., Smith, K.A., Kolb, C.E. and Worsnop, D.R. (2000): Development of aerosol mass Spectrometer for Size and Composition Analysis of Submicron Particle, aerosol Science and Technology, 33, 49-70.

Jokinen, T., Sipilä, M., Junninen, H., Ehn, M., Lönn, G., Hakala, J., Petäjä, T., Mauldin III, R.L., Kulmala, M. and Worsnop, D.R. (2012): Atmospheric sulfuric acid and neutral cluster measurements using CI-APi-TOF, Atmos. Chem. Phys. 12, 4117-4125.

Junninen, H., Ehn, M., Petäjä, T., Luosujärvi, L., Kotiaho, T., Kostiainen, R., Rohner, U., Gonin, M., Fuhrer, K., Kulmala, M. and Worsnop, D.R. (2010): API-ToFMS: a tool to analyze composition of ambient small ions. Atmos. Meas. Technol., 3, pp. 1039-1053.

Karppinen, A. and Johansson, L. (2018): Fusion of Air Quality Information: Evaluation of the Enfuser-Methdoology in Finland and a Case Study in China. Air Pollution Modeling and its Application XXV. Ed. by C. Mensink and G. Kallos. Cham: Springer International Publishing, 213–218.

Kaski, N., Loukkola, K., Portin, H. (2017): Air quality in the Helsinki metropolitan area in 2016. (in Finnish, abstract in English) HSY publications 3/2017.

Kontkanen, J., Paasonen, P., Aalto, J., Bäck, J., Rantala, P., Petäjä, T., and Kulmala, M. (2016): Simple proxies for estimating the concentrations of monoterpenes and their oxidation products at a boreal forest site, Atmos. Chem. Phys., 16, 13291-13307, https://doi.org/10.5194/acp-16-13291-2016.

Kukkonen, J.K., Karl, M.K., Keuken, M.P., Denier van der Gon, H.A.C., Denby, B.R., Singh, V., Douros, J., Manders, A., Samaras, Z., Moussiopoulos, N., Jonkers, S., Aarnio, M., Karppinen, A., Kangas, L., Lützenkirchen, S., Petäjä, T., Vouitsis, I. and Sokhi, R.S. (2016): Modelling the dispersion of particle numbers in five European cities, Geosci. Model. Dev. 9, 451-478.

Kulmala, M., Petäjä, T., Ehn, M., Thornton, J., Sipilä, M., Worsnop, D.R. and Kerminen, V.-M. (2014): Chemistry of atmospheric nucleation: On the recent advances on precursor characterization and atmospheric cluster composition in connection with atmospheric new particle formation, Annu. Rev. Phys. Chem. 65, 21-37.

Kulmala, M., Petäjä, T., Kerminen, V.-M., Kujansuu, J., Ruuskanen, T., Ding, A.J., Nie, W., Hu, M., Wang, Z.B., Wu, Z.J., Wang, L., and Worsnop, D.R. (2016): On secondary new particle formation in China, Front. Env. Sci. Eng. 10, 08, doi: 10.1007/s11783-016-0850-1.

Mikkonen, S., Romakkaniemi, S., Smith, J. N., Korhonen, H., Petäjä, T., Plass-Duelmer, C., Boy, M., McMurry, P. H., Lehtinen, K. E. J., Joutsensaari, J., Hamed, A., Mauldin III, R. L., Birmili, W., Spindler, G., Arnold, F., Kulmala, M., and Laaksonen, A. (2011): A statistical proxy for sulphuric acid concentration, Atmos. Chem. Phys., 11, 11319–11334, doi:10.5194/acp-11-11319-2011.

Moltchanov, S., Levy, I., Etzion, Y., Lerner, E., Broday, D.M. and Fishbain, B. (2015): On the feasibility of measuring urban air pollution by wireless distributed sensor networks, Sci. Tot. Environ. 502, 537-547.

Ng, N. L., Herndon, S. C., Trimborn, A., Canagaratna, M. R., Croteau, P. L., Onasch, T. B., Sueper, D., Worsnop, D. R., Zhang, Q., Sun, Y. L., and Jayne, J. T. (2011): An Aerosol Chemical Speciation Monitor (ACSM) for Routine Monitoring of the Composition and Mass Concentrations of Ambient Aerosol, Aerosol Science and Technology, 45, 780-794, 10.1080/02786826.2011.560211.

Onasch, T. B., Trimborn, A., Fortner, E. C., Jayne, J. T., Kok, G. L., Williams, L. R., Davidovits, P., and Worsnop, D. R. (2012): Soot Particle Aerosol Mass Spectrometer: Development, Validation, and Initial Application, Aerosol Science and Technology, 46, 804-817, 10.1080/02786826.2012.663948.

Paasonen, P., Nieminen, T., Asmi, E., Manninen, H. E., Petäjä, T., Plass-Dülmer, C., Flentje, H., Birmili, W., Wiedensohler, A., Hõrrak, U., Metzger, A., Hamed, A., Laaksonen, A., Facchini, M. C., Kerminen, V.-M., and Kulmala, M. (2010): On the roles of sulphuric acid and low-volatility organic vapours in the initial steps of atmospheric new particle formation, Atmos. Chem. Phys., 10, 11223-11242, https://doi.org/10.5194/acp-10-11223-2010.

Petäjä, T., Mauldin III, R.L., Kosciuch, E., McGrath, J., Nieminen, T., Adamov, A., Kotiaho, T. and Kulmala, M. (2009): Sulfuric acid and OH concentrations in a boreal forest site, Atmos. Chem. Phys. 9, pp. 7435-7448.

Saarikoski, S., Sillanpää, M., Sofiev, M., Timonen, H., Saarnio, K., Teinilä, K., Karppinen, A., Kukkonen, J., and Hillamo, R. (2007): Chemical composition of aerosols during a major biomass burning episode over northern Europe in spring 2006: Experimental and modelling assessments, Atmospheric Environment, 41, 3577-3589, 10.1016/j.atmosenv.2006.12.053.

Saarikoski, S., Timonen, H., Saarnio, K., Aurela, M., Jarvi, L., Keronen, P., Kerminen, V. M., and Hillamo, R. (2008): Sources of organic carbon in fine particulate matter in northern European urban air, Atmospheric Chemistry and Physics, 8, 6281-6295.

Saffari, A., Hasheminassab, S., Wang, S., Shafer, M.M., Schauer, J.J. and Sioutas, C. (2015): Impact of primary and secondary organic sources on the oxidative potential of quasi-ultrafine particles (PM0.25) at three contrasting locations in the Los Angeles Basin, Atmos. Environ. 120, 286-296.

Sipilä, M., Sarnela, N., Jokinen, T., Junninen, H., Hakala, J., Rissanen, M.P., Praplan, A.P., Simon, M., Kürten, A., Bianchi, F., Dommen, J., Curtius, J., Petäjä, T. and Worsnop, D.R. (2015): Bisulphate-cluster based atmospheric pressure chemical ionization mass spectrometer for high sensitivity (<100 ppqV) detection of atmospheric dimethyl amine: proof-of-concept and first ambient data from boreal forest, Atmos. Meas. Technol. 8, 4001-4011.

Timonen, H., Carbone, S., Aurela, M., Saarnio, K., Saarikoski, S., Ng, N. L., Canagaratna, M. R., Kulmala, M., Kerminen, V. M., Worsnop, D. R., and Hillamo, R. (2013): Characteristics, sources and water-solubility of ambient submicron organic aerosol in springtime in Helsinki, Finland, Journal of Aerosol Science, 56, 61-77, 10.1016/j.jaerosci.2012.06.005.

von Bismarck-Osten, C., Birmili, W., Ketzel, M., Massling, A., Petäjä, T. and Weber, S. (2013): Characterization of parameters influencing the spatio-temporal variability of urban particle number size distributions in four European cities, Atmos. Environ. 77, 415-429.

von Klot, S., Peters, A., Aalto, P., Bellander, T., Berglind, N., D'Ippoliti, D., Elosua, R., Hörmann, A., Kulmala, M., Lanki, T., Löwel, H., Pekkanen, J., Picciotto, S., Sunyer, J. and Forastiere, F. (2005):

Ambient air pollution is associated with increased risk of hospital cardiac readmissions of myocardial infarction survivors in five European cities, Circulation 112, 3073-3079

Wu, Y., Häkkinen, E., Cai, R., Enroth, J., Petäjä, T., Kulmala, M., Kangasluoma, J. (2019): Small, autonomous and low maintenance CPC for ultrafine particle monitoring networks. *Manuscript in preparation*